

# Congo red interactions with curli-producing *E. coli* and native curli amyloid fibers

Courtney Reichhardt<sup>1,‡</sup>, Amy N. Jacobson<sup>1,‡</sup>, Marie C. Maher<sup>1</sup>, Jeremy Uang<sup>1</sup>, Oscar A. McCrate<sup>1</sup>, Michael Eckart<sup>2</sup>, and Lynette Cegelski<sup>\*1</sup>

<sup>1</sup>*Department of Chemistry, Stanford University, Stanford, CA 94305*

<sup>2</sup>*Protein and Nucleic Acid Facility, Stanford University, Stanford, CA 94305*

<sup>‡</sup>These authors contributed equally to this work.

**Keywords:** curli; functional amyloid; amyloid; Congo red; amyloid dye; surface plasmon resonance; *E. coli*

**Contact Information:** cegelski@stanford.edu

## ABSTRACT

Microorganisms produce functional amyloids that can be examined and manipulated *in vivo* and *in vitro*. *Escherichia coli* assemble extracellular adhesive amyloid fibers termed curli that mediate adhesion and promote biofilm formation. We have characterized the dye binding properties of the hallmark amyloid dye, Congo red, with curliated *E. coli* and with isolated curli fibers. Congo red binds to curliated whole cells, does not inhibit growth, and can be used to comparatively quantify whole-cell curliation. Using Surface Plasmon Resonance, we measured the binding and dissociation kinetics of Congo red to curli. Furthermore, we determined that the binding of Congo red to curli is pH-dependent and that histidine residues in the CsgA protein do not influence Congo red binding. Our results on *E. coli* strain MC4100, the most commonly employed strain for studies of *E. coli* amyloid biogenesis, provide a starting point from which to compare the influence of Congo red binding in other *E. coli* strains and amyloid-producing organisms.

## INTRODUCTION

*E. coli* and *Salmonella* species assemble extracellular adhesive amyloid fibers termed curli that mediate cell-surface and cell-cell interactions and serve as an adhesive and structural scaffold to promote biofilm assembly and other community behaviors(1-4). Curli are among a growing list of functional microbial amyloids that emphasize Nature's ability to coordinate the assembly of amyloid fibers to promote community behavior and function. Amyloid fibers contribute to sporulation in *Streptomyces*(5) and to adhesion and biofilm formation in *E. coli*(1, 4) as well as in *Salmonella*(2) species, *B. subtilis*(6), *S. aureus*(7), and *S. mutans*(8), and others(8, 9). Curli and other amyloid fibers have important roles in modulating the viscoelastic properties of biofilms. This property has been identified in rheological studies of natively produced curli-containing pellicle (biofilm formed at the air-liquid interface) (10) and in studies of *in vitro* formed biofilm-like materials (11). In *E. coli*, curli biogenesis requires specific molecular machinery encoded by the *csgBA* and *csgDEFG* operons(3). *In vivo* polymerization of the major curli subunit CsgA into  $\beta$ -sheet-rich amyloid fibers requires the nucleator protein, CsgB(3). CsgG is an outer membrane protein(12) and CsgE and CsgF are assembly factors required for the stabilization and transport of CsgA and CsgB to the cell surface(13,14). Thus, in contrast to the undesired and alternative protein folding events that lead to amyloid formation in human amyloid diseases including Alzheimer's, Parkinson's, and Huntington's diseases(15), bacteria harness dedicated machinery in order to direct the assembly of amyloid fibers at their cell surface for function.

As amyloid, curli share some general structural, biochemical, and biophysical properties with other functional amyloids and disease-related amyloids. Structurally, amyloid fibers are comprised of polypeptides rich in  $\beta$ -sheet secondary structure in which individual  $\beta$ -strands are primarily aligned perpendicular to the fiber axis(16,17). Amyloid fibers share biochemical properties: they are resistant to SDS(18) and proteases(19) and they bind the classic amyloid dyes, Congo red (CR) and thioflavin T(20). CR was the dye first used to identify amyloid in tissue specimens and remains a benchmark to identify the presence of amyloid through its detectable fluorescence upon binding to amyloid or its birefringence under polarized light. CR binding to  $\beta$ -amyloid has been studied extensively and reviewed recently, and it is used to ultimately confirm diagnoses of Alzheimer's diseases through post-mortem staining of brain tissue(21).

Curli production among *E. coli* and *Salmonella* strains is often scored qualitatively by the staining of colonies grown in the presence of CR. However, because CR can bind to other cellular features in some bacterial strains including cellulose, care must be taken to consider dye binding as a reliable indicator of amyloid production only among bacterial strains that exhibit curli-dependent CR binding, *i.e.* among strains in which curli mutations abolish CR binding(22). In this way, CR-binding phenotypes have been valuable in studies of curli biogenesis in MC4100, the most well studied *E. coli* strain for dissecting curli biogenesis(3). MC4100 produces curli localized at the cell surface. When grown on CR-containing nutrient agar medium, curliated whole cells bind CR and deplete the dye from the underlying agar. Deletion of the curli chaperone-like protein, CsgF, on the other hand, results in aberrant assembly and fiber mislocalization(12). In the *csgF* mutant, CR binding is observed in the underlying agar after cells

are removed from the agar, which is attributed to the mislocalization of curli fibers away from the cell surface(12). This phenotype, as well as other phenotypes ascribed to fibers formed in modified genetic backgrounds, has improved our model of curli assembly and the multi-protein curli machinery. The coordinated assembly process emphasizes the importance of examining the structural and biochemical properties of curli when formed natively by *E. coli*, when possible, rather than using curli-like fibers polymerized *in vitro* from purified preparations of the major fiber subunit protein, CsgA. Thus, we examined the interactions of curliated whole cells and native curli with the amyloid dye CR.

## RESULTS AND DISCUSSION

CR has been used extensively to supplement nutrient agar as a selection medium to distinguish curli-producing bacteria from non-curliated bacteria when CR-binding is confirmed to be curli-dependent (Fig. 1A). Final CR concentrations in indicator plates are typically 10-30 µg/mL. We determined that bacterial growth in CR-containing agar medium with final CR concentrations as high as 200 µg/mL did not alter curli production, as assessed by immunoblot analysis with the detection of CsgA and CsgG protein levels of whole-cell samples normalized by cell number (Fig. 1B). This assay was also performed for a panel of uropathogenic *E. coli*, and we similarly found that CR did not inhibit curli fibrillation for these other clinically relevant *E. coli* strains (Fig. S1). Western blot analysis as a function of growth time also revealed that CR does not influence the kinetics of curli production *in vivo* (Fig. 1C). The appreciated time-dependence of curli production on agar can be noted in the curli protein Western blot profiling, where curli production is upregulated as cell density increases from 6 through 36 hours. Thus, although CR

has been shown to inhibit the formation of amyloid fibers by some amyloidogenic proteins *in vitro*(23), we demonstrate that CR does not inhibit the biogenesis of curli *in vivo* during growth on YESCA agar.

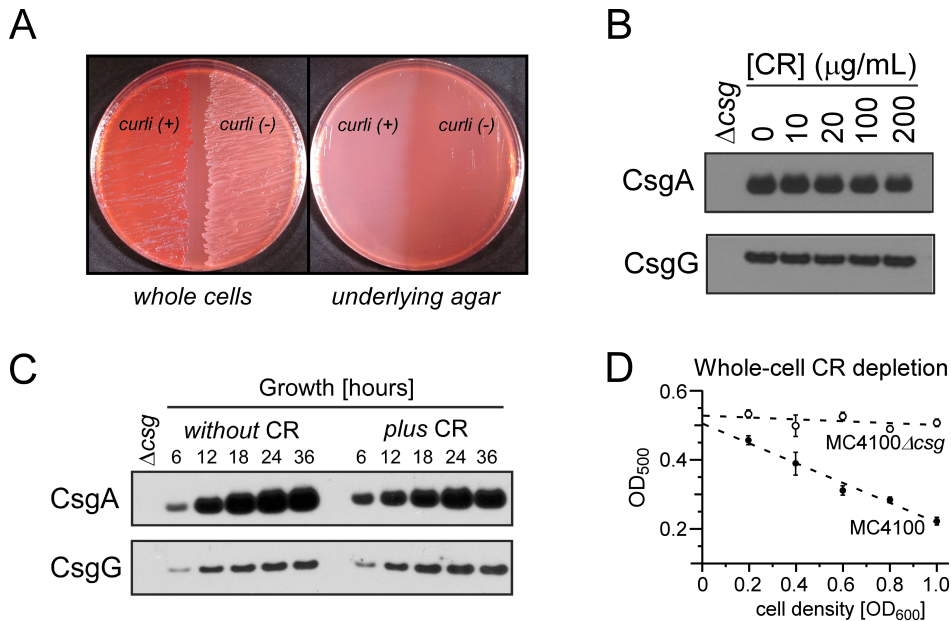


**Figure 1**

**Figure 1. Congo red and *E. coli*.** (A) Curli-producing *E. coli* bind CR when growing on CR-supplemented nutrient agar (left). The depletion of CR from the underlying agar can be observed when cells are removed from the growth plate (right). (B) Supplementation of the agar with CR at concentrations of up to 200  $\mu$ g/mL does not affect curli production on a per cell basis as assessed by Western blot analysis. CsgA is the main curli fiber subunit and CsgG oligomerizes in the outer membrane to form a pore for the transport of curli subunits to the cell surface. (C) Supplementation of the agar with CR also does not influence the typical kinetics of curli production, where more curli are produced as cells enter the stationary phase. (D) A whole-cell CR depletion assay provides a way to evaluate and compare curli production among MC4100 samples. Bacteria were incubated with 10  $\mu$ g/mL CR and the extent of free CR in the supernatant after centrifugation of CR-bound whole cells was monitored by UV-Vis spectrophotometry. CR depletion from the supernatant is enhanced in a linear fashion as the number of cells and amount of curli are increased. Error bars correspond to the standard deviation of measurements for three separate samples.

Curliated whole cells grown normally on YESCA agar without CR have been noted for their ability to bind CR upon incubation with a CR solution(24,25). We characterized this phenomenon quantitatively using MC4100 whole cells. Increases in CR depletion tracked linearly with bacterial concentration (Fig. 1D). As the density of MC4100 was increased, more CR was depleted from the solution. Curli mutant cells, MC4100Δcsg, did not exhibit significant CR binding and depletion. Thus, relative cell-associated curli levels in MC4100 can be determined by a CR depletion assay. This provides a convenient and rapid way to assay and compare curli production across whole-cell samples that may be advantageous as a higher throughput assay without requiring immunoblotting or fiber purification protocols.

Previous studies with isolated native curli(3) and other amyloid fibers, notably  $\beta$ -amyloid(26), have demonstrated the absorbance and fluorescence spectral changes that occur when CR binds to curli and amyloids. UV-Vis spectra exhibit an increase in CR intensity and a red shift when CR is bound to curli (3). In addition, CR exhibits very little detectable fluorescence in solution, but fluoresces when bound to curli (3,22). We extended the biophysical analyses of native curli to examine CR binding using Surface Plasmon Resonance (SPR).

The use of SPR to examine the binding of CR to curli required the identification of a suitable regeneration condition in order to remove CR from immobilized fibers after compound association and dissociation events during the SPR measurement (Fig. S2). Of all the conditions tested to remove CR bound to native curli fibers, a few successful regeneration conditions were identified: 100% DMSO; 50% DMSO/10 mM NaOH; and 100% DMF. Conditions that did not remove CR from curli fibers included: acetone, dichloromethane, ethyl acetate, 2-propanol, tetrahydrofuran, and toluene. Additionally, a solution of 100 mM HCl that was employed for the

regeneration of curli-like fibers fibrillized *in vitro*(27) was not sufficient to remove CR from our native curli fibers. We selected 50%DMSO/10mM NaOH as the regeneration condition for our SPR experiments as it was most compatible with the SPR instrument and protocols.

The association and dissociation kinetics of CR as a function of concentration are presented in Figure 2A. CR association gradually increased during the association phase from 0 to 150 s as CR was introduced at the specified concentration through continuous flow over immobilized curli fibers on the SPR chip for the duration of the association phase (Fig. 2A). During the dissociation phase, CR was not present in the buffer and a gradual decline in response units (RU) during the next 150 s revealed the dissociation of CR from the immobilized fibers, yielding a final residual response of about 50 RU. Thus, a fraction of CR remained bound to curli and was only removed after the regeneration step. The complete removal of CR and regeneration of curli was achieved with a solution of 50%DMSO/10mM NaOH. Binding to curli was unaffected by repeated regeneration and identical response curves were obtained whether the experiments were performed as a function of increasing or decreasing CR concentration. The equilibrium binding constant was obtained using the Langmuir model ( $A+L \rightleftharpoons AL$ ) by non-linear curve fitting of the Langmuir binding isotherm,  $R_{eq} = (k_a [A]/(k_a [A] + K_d)) * R_{max}$ , where  $R_{eq}$  is the shift in SPR angle at equilibrium (or “Response units”, RU) and  $R_{max}$  is the maximum analyte binding capacity of the surface in RU. The equilibrium constant,  $K_d$ , for CR binding to curli was determined to be 2.8  $\mu$ M, as calculated from the association and dissociation rates. This value is similar to those reported for CR binding to other amyloids including A $\beta$ 11-28 (1-10  $\mu$ M)(28).

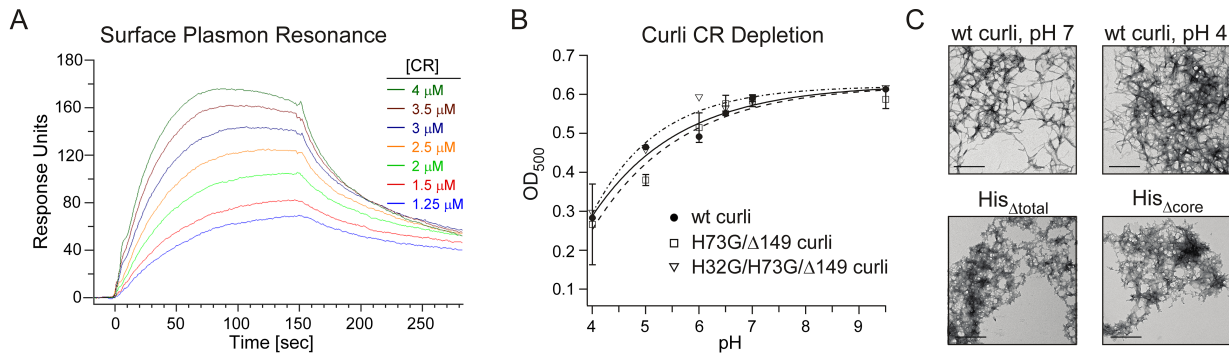


Figure 2

**Figure 2. Interactions of CR with isolated curli.** (A) Surface plasmon resonance experiments performed with immobilized curli revealed that CR binding is relatively weak; CR binds to curli with an approximate  $k_d$  of 2.8  $\mu\text{M}$ . (B) A CR depletion assay allowed facile examination of CR binding to isolated curli, similar to the whole-cell assay performed in Fig. 1. The data demonstrate that CR binding to curli is pH dependent and is not dependent on histidine in the CsgA sequence. (C) Curli produced by wild-type MC4100 are comparable to those formed by the histidine mutants and are not influenced by changes in pH, as demonstrated by electron microscopy.

CR binding to  $\beta$ -amyloid fibers formed *in vitro* has been reported to be pH-dependent(28). To determine if CR binding to curli fibers displayed a similar pH-dependence, we adapted the whole-cell CR depletion assay to monitor the depletion of CR resulting from CR binding to isolated curli rather than using whole cells, which would not tolerate extreme pH conditions. Solutions of 0.1 mg/mL curli at pH values of 4 to 9.5 (in 80% ethanol) were incubated with 10  $\mu\text{g}/\text{mL}$  CR followed by centrifugation to pellet curli and bound CR. Free CR in the supernatant was monitored by UV-Vis spectrophotometry. More CR bound to curli at lower pH values, and CR binding decreased, with more free CR present in the supernatant, as pH values increased from 6 to 9.5 (Fig. 2B). Selection of ethanol in the assay was based upon its use in histological screens and assays(28,29). The general morphology of curli fibers in 80% (v/v) ethanol was not

affected as determined by TEM (Fig. 2C).

The pH dependence of CR binding to curli is similar to the proton dissociation curve for histidine, and CR binding to  $\beta$ -amyloid fibers formed *in vitro* has been shown to be dependent on the presence of histidine in the protein sequence(30). Thus, we tested whether histidine might underlie Congo red binding in curli using curli isolated from cells producing: (i) wild type CsgA (as above); (ii) CsgA lacking histidine residues only within the proposed amyloid core (H73G/ $\beta$ 149), curli $\beta$ His<sub>core</sub>; and (iii) CsgA lacking histidine residues in both the proposed amyloid core and the N-terminus (H32G/H73G/ $\beta$ 149), curli $\beta$ His<sub>total</sub>. CsgA contains an N-terminal sec signal sequence that is removed upon secretion into the periplasm. Following this, the next N-terminal 22 amino acids are protease sensitive and not thought to be part of the CsgA amyloid core, and includes His32. The proposed amyloid core consists of residues 43-151(31). As demonstrated in Figure 2B, CR binding to curli fibers isolated from the histidine mutants was comparable to the binding to wild-type fibers. Electron micrographs confirmed that the mutant CsgA proteins assembled into amyloid fibers, although they were somewhat shorter in length from curli isolated from MC4100 (Fig. 2C). We note that in the curli preparations, the yield of curli isolated from the His mutants was considerably lower than that of wild type curli isolated from MC4100. Thus, in the His mutants, a preparation using cell lysates was employed to access fibers that still remained cell-associated, whereas a more gentle application of shear forces is sufficient to remove wild-type curli from MC4100.

In summary, CR has been used extensively in microbiological studies to score the production of microbial amyloids as well as polysaccharides and other extracellular factors. However, there is little detail available regarding how CR binds to microbial amyloid fibers. Furthermore, CR

inhibits the fibrillization of some amyloidogenic proteins, such as  $\beta$ -amyloid(23), in *in vitro* amyloid polymerization assays. Yet, in microbial systems such as *E. coli* and *Salmonella*, CR has not appeared to inhibit amyloid biogenesis *in vivo*. Here, we have demonstrated quantitatively that CR does not inhibit the production of curli in *E. coli* when supplemented in nutrient agar at concentrations up to 200  $\mu$ g/mL, and does not influence the kinetics of curli production.

A tractable feature of microbial amyloids is the presentation of amyloid fibers at the cell surface. Such extracellular display permits facile identification and visualization by electron microscopy, simple whole-cell amyloid-staining using CR or other dyes, and relatively straightforward isolation and purification. Thus, fibers and fiber-dye or fiber-protein complexes can be readily examined using fibers formed natively in their cellular context. Using SPR, we demonstrated that CR binds to immobilized curli with an approximate  $K_d$  of 2.8 uM. We also discovered that CR binding to curli is pH dependent and is not histidine dependent. This is consistent with a previous study that demonstrated that a synthetic short peptide related to a fragment of CsgA still polymerized and would bind CR despite not containing histidine (32). Other curli residues may play a role in CR binding to curli such as the aromatic amino acids phenylalanine and tryptophan that may interact with the phenolic rings in CR(33). In contrast, lysine was shown to be required for CR binding to the fungal prion Het-S(34). Our comparative analysis on the influence of CR with curliated *E. coli* and isolated curli formed natively *in vivo* provides a benchmark from which to compare other curli-binding molecules, mutant curli fibers, curli-type fibers formed through *in vitro* polymerizations, and other functional bacterial amyloids formed *in vivo*.

## Methods

*Curli-associated E. coli sample preparation.* Bacteria were grown on YESCA (0.5g/L yeast extract; 10g/L casamino acids) agar plates in the presence or absence of CR at 26 °C. A CR (MP Biomedicals, LLC, Cat# 150711, Lot# MR30568) stock solution was prepared as 2 mg/mL in water and sterile-filtered. Designated volumes of CR were added to stirring hot agar medium to achieve the desired final concentration before pouring standard plates (approximately 25mL media per 100 mm petri plate). For the photographed plate in Figure 1A, MC4100 were grown for 48 hours at 26 °C on YESCA agar containing 25 $\mu$ g/mL CR.

*Western blot analysis.* The cell-associated curli proteins, CsgA and CsgG, were examined by immunoblot assays as described (35). Whole-cell samples with equivalent cell number were prepared as cell pellets of 1mL cell culture with an OD<sub>600</sub> of 1.0. Each pellet was treated with 100  $\mu$ L hexafluoroisopropanol (HFIP) or formic acid (FA), as indicated, to dissociate curli subunits. HFIP or FA was removed by vacuum centrifugation, and samples were resuspended in SDS-PAGE loading buffer. Protein gel electrophoresis was carried out using 12% SDS-PAGE gels (Invitrogen). Proteins were transferred to 0.2  $\mu$ m nitrocellulose transfer membranes (Whatman). The polyclonal rabbit antiserum to CsgA or CsgG was used as the primary antibody and horseradish peroxidase (HRP) conjugated goat anti-rabbit antibody (Pierce) was used as the secondary antibody (36).

*Whole-cell Congo red depletion assay.* Whole-cell samples were suspended in ice-cold PBS as a dilution series with OD<sub>600</sub> of 0.2 to 1.0, and CR was added to a final concentration of 10  $\mu$ g/mL from a filtered stock solution of 1 mg/mL. The cells were incubated with CR for 10 minutes at

room temperature with rocking. The cells were pelleted (10,000 g for 5 minutes), and the absorbance at 500 nm of the supernatant was measured. For all absorbance experiments, a cell path length of 1 cm was used (Perkin Elmer Lambda 35 UV/Vis Spectrometer). Each sample was prepared and assayed in triplicate. Error bars correspond to the standard deviation of measurements for three separate samples.

*Surface Plasmon Resonance (SPR)-based Biosensor Analysis.* The interaction of CR and fibronectin with curli fibers was analyzed by Surface Plasmon Resonance using a BIACORE 3000 biosensor system (GE Healthcare). Analyte (CR or Fibronectin) dilutions were performed in HBS-EP (10 mM HEPES, pH 7.4, 150 mM NaCl, 3mM EDTA, and 0.005% v/v Surfactant P20) running buffer. Curli were immobilized onto a CM5 biosensor chip by amine coupling chemistry using N-hydroxysuccinimide (NHS) and N’-(3-dimethylaminopropyl) carbodiimide hydrochloride (EDC). To investigate binding of CR and Fibronectin, the diluted analytes were injected over the curli fiber surface. The experiments were performed at 25 °C using a flow rate of 50 L/min. For each experiment, at least 5 different concentrations of CR or Fibronectin were injected over each experimental and control flow cell for 150 sec. Dissociation was allowed to occur at the same flow rate for 180 sec in Running Buffer alone. The surface was regenerated after each injection of analyte using two 18 sec pulses of 50% DMSO/ 10mM NaOH which led to complete dissociation of the residually bound CR and fibronectin. All data were corrected for non-specific binding by subtracting the signal measured in a control cell lacking immobilized ligand. Both data processing and kinetic fitting were performed using Scrubber software, version 2 (BioLogic Software, Pty., Australia) or BIAevaluation software 4.1 (Biacore).

*Curli production and isolation.* Wild-type curli were isolated from YESCA-agar grown MC4100 as previously described<sup>7</sup>. To obtain CsgA lacking histidines or lacking only core histidines, appropriate plasmids (pMC3-H32G-H73G-□149 and pMC3-H73G-□149, respectively) were generated using pMC3 (Chapman Laboratory) as a template (GenScript, New Jersey, USA). Protein expression was performed in *E.coli* strain LSR12 grown in Luria broth at 37°C. Protein expression was induced with 0.25 mM ITPG for 60 minutes when cell densities reached an OD<sub>600</sub> of ~1. Cells were harvested by centrifugation (10,000 g, 20 minutes, 4°C). The cell pellet was frozen and then resuspended in lysis buffer (8 M GdnHCl). Cells were lysed by sonication (6x 10 s bursts with 15 s cooling period on ice between each burst) and centrifuged (10,000 g, 20 minutes, 4°C) to remove cellular debris. The supernatant was dialyzed overnight against 50 mM Na<sub>2</sub>HPO<sub>4</sub> (3.5 MWCO), and then centrifuged (13,000 g, 30 minutes, 20°C). The pellet was resuspended in 10 mM Tris, pH 7.4 with 4% (w/v) final concentration SDS and incubated overnight, rocking at room temperature. The CsgA-H73G-□149 fibrils were initially pelleted (13,000 g, 60 minutes, 20°C) and then resuspended in 10 mM Tris (pH 7.4). The curli were pelleted again (30,000 g, 30 minutes, 20°C) and resuspended in 10 mM Tris (pH 7.4); this final washing step was repeated approximately four times until the SDS was removed. The final curli pellet was resuspended in 5 mL of water. The concentration of the curli solution was determined using the BCA Protein Assay (Thermo Scientific Pierce BCA Protein Assay Kit). CR was quantified by measuring the absorbance at 500 nm in 10 mM Tris-HCl at pH 7.5, with an extinction coefficient of 5 x 10<sup>4</sup> M<sup>-1</sup> cm<sup>-1</sup>.

*Transmission electron microscopy (TEM).* Negative staining TEM was performed on curli samples. Samples were applied to 300-mesh copper grids coated with Formvar film (Electron

Microscopy Sciences, Hatfield, PA) for 2 min, rinsed in deionized water, negatively stained with 2% uranyl acetate for 90 s, and air-dried. Microscopy was performed on the JEM-1400 (JEOL, LLC).

*Curli-only Congo red depletion assay.* Curli (0.1 mg/mL) were suspended in solutions of nominal pH values of 4 to 9.5, in 80% (v/v) ethanol and 5 mM buffer (glycine at pH 4.0 and 5.0; 4-morpholineethanesulfonic acid (MES) at pH 6.0 and 6.5; and Tris(hydroxymethyl)-aminomethane (TRIS) at pH 7.0 and 9.5). For the pH-dependence assays, curli (0.1 mg/mL) were incubated with 10 µg/mL CR (from 1 mg/mL aqueous stock solution) for 10 minutes, rocking at room temperature before centrifugation (13,000 g for 10 minutes) to remove curli and bound CR. The supernatant absorbance was measured at 500 nm. Each sample was prepared and assayed in triplicate with the exception of CsgA-H32G-H73G-Δ149 fibrils, which was only a single sample due to limited sample size. Error bars correspond to the standard deviation of measurements for three separate samples.

## REFERENCES

1. Olsen A, Jonsson A, Normark S. Fibronectin binding mediated by a novel class of surface organelles on *Escherichia coli*. *Nature*. 1989;338(6217):652-5.
2. Collinson SK, Emody L, Muller KH, Trust TJ, Kay WW. Purification and characterization of thin, aggregative fimbriae from *Salmonella enteritidis*. *J Bacteriol*. 1991;173(15):4773-81.
3. Chapman MR, Robinson LS, Pinkner JS, Roth R, Heuser J, Hammar M, et al. Role of *Escherichia coli* curli operons in directing amyloid fiber formation. *Science*. 2002;295(5556):851-5.
4. Barnhart MM, Chapman MR. Curli biogenesis and function. *Annu Rev Microbiol*. 2006;60:131-47.

5. Capstick DS, Jomaa A, Hanke C, Ortega J, Elliot MA. Dual amyloid domains promote differential functioning of the chaplin proteins during *Streptomyces* aerial morphogenesis. *Proc Natl Acad Sci USA*. 2011;108(24):9821-6.
6. Romero D, Aguilar C, Losick R, Kolter R. Amyloid fibers provide structural integrity to *Bacillus subtilis* biofilms. *Proc Natl Acad Sci USA*. 2010;107(5):2230-4.
7. Schwartz K, Syed AK, Stephenson RE, Rickard AH, Boles BR. Functional Amyloids Composed of Phenol Soluble Modulins Stabilize *Staphylococcus aureus* Biofilms. *Plos Pathog*. 2012;8(6).
8. Alteri CJ, Xicohtencatl-Cortes J, Hess S, Caballero-Olin G, Giron JA, Friedman RL. *Mycobacterium tuberculosis* produces pili during human infection. *Proc Natl Acad Sci USA*. 2007;104(12):5145-50.
9. Dueholm MS, Petersen SV, Sonderkaer M, Larsen P, Christiansen G, Hein KL, et al. Functional amyloid in *Pseudomonas*. *Mol Microbiol*. 2010. 77, 1009-1020.
10. Wu C, Lim JY, Fuller GG, Cegelski L. Quantitative analysis of amyloid-integrated biofilms formed by uropathogenic *Escherichia coli* at the air-liquid interface. *Biophys J*. 2012;103(3):464-71.
11. Lembré P, Di Martino P, Vendrely C. Amyloid peptides derived from CsgA and FapC modify the viscoelastic properties of biofilm model matrices. *Biofouling*. 2014;30(4):415-426.
12. Goyal P, Krasteva PV, Van Genven N, Gubellini F, Van den Broeck I, Troupiotis-Tsailaki A, et al. Structural and mechanistic insights into the bacterial amyloid secretion channel CsgG. *Nature*. 2014;516(7530):250-3.
13. Robinson LS, Ashman EM, Hultgren SJ, Chapman MR. Secretion of curli fibre subunits is mediated by the outer membrane-localized CsgG protein. *Mol Microbiol*. 2006;59(3):870-81.
14. Nenninger AA, Robinson LS, Hultgren SJ. Localized and efficient curli nucleation requires the chaperone-like amyloid assembly protein CsgF. *Proc Natl Acad Sci USA*. 2009;106(3):900-5.
15. Chiti F, Dobson CM. Protein misfolding, functional amyloid, and human disease. *Annu Rev Biochem*. 2006;75:333-66.
16. Eanes ED, Glenner GG. X-Ray Diffraction Studies on Amyloid Filaments. *J Histochem Cytochem*. 1968;16(11):673-7.
17. Bonar L, Cohen AS, Skinner MM. Characterization of Amyloid Fibril as a Cross-Beta Protein. *P Soc Exp Biol Med*. 1969;131(4):1373-5.
18. Manning M, Colon W. Structural basis of protein kinetic stability: Resistance to sodium dodecyl sulfate suggests a central role for rigidity and a bias toward beta-sheet structure. *Biochemistry-US*. 2004;43(35):11248-54.
19. Sipe JD. Amyloidosis. *Annu Rev Biochem*. 1992;61:947-75.
20. Westermark GT, Johnson KH, Westermark P. Staining methods for identification of amyloid in tissue. *Amyloid, Prions, and Other Protein Aggregates*. 1999;309:3-25.
21. Reinke AA, Gestwicki JE. Insight into amyloid structure using chemical probes. *Chem Biol Drug Des*. 77(6):399-411.
22. McCrate OA, Zhou X, Cegelski L. Curcumin as an Amyloid-indicator Dye in *E. coli*. *Chemical Communications*. 2013; 49: 4193-4195.
23. Podlisny MB, Walsh DM, Amarante P, Ostaszewski BL, Stimson ER, Maggio JE, et al. Oligomerization of Endogenous and Synthetic Amyloid Beta-Protein at Nanomolar Levels in Cell Culture and Stabilization of Monomer by Congo Red. *Biochemistry-US*. 1998;37:3602-11.

24. Gophna U, Barlev M, Seijffers R, Oelschlager TA, Hacker J, Ron EZ. Curli fibers mediate internalization of *Escherichia coli* by eukaryotic cells. *Infect Immun.* 2001;69(4):2659-65.

25. Cherny I, Rockah L, Levy-Nissenbaum O, Gophna U, Ron EZ, Gazit E. The formation of *Escherichia coli* curli amyloid fibrils is mediated by prion-like peptide repeats. *J Mol Biol.* 2005;352(2):245-52.

26. Klunk WE, Jacob RF, Mason RP. Quantifying amyloid by Congo red spectral shift assay. *Method Enzymol.* 1999;309:285-305.

27. Kai-Larsen Y, Luthje P, Chromek M, Peters V, Wang X, Holm A, et al. Uropathogenic *Escherichia coli* modulates immune responses and its curli fimbriae interact with the antimicrobial peptide LL-37. *Plos Pathog.* 6(7):e1001010.

28. Inouye H, Nguyen J, Fraser P, Shinchuk L, Packard A, Kirschner D. Histidine residues underlie Congo red binding to A beta analogs. *Amyloid.* 2000;7(3):179-88.

29. Eisert R, Felau L, Brown LR. Methods for enhancing the accuracy and reproducibility of Congo red and thioflavin T assays. *Analytical biochemistry.* 2006;353(1):144-6.

30. Inouye H, Nguyen JT, Fraser PE, Shinchuk LM, Packard AB, Kirschner DA. Histidine residues underlie Congo red binding to A beta analogs. *Amyloid-International Journal of Experimental and Clinical Investigation.* 2000;7(3):179-88.

31. Wang X, Smith DR, Jones JW, Chapman MR. In vitro polymerization of a functional *Escherichia coli* amyloid protein. *The Journal of biological chemistry.* 2007;282(6):3713-9.

32. Lembré P, Vendrelé C, Di Martino P. Amyloid Fiber Formation by Synthetic Peptides Derived from the Sequence of the Protein CsgA of *Escherichia coli*. *Prot Pept Lett.* 2013;20:942-946.

33. Porat Y, Abramowitz A, Gazit E. Inhibition of amyloid fibril formation by polyphenols: structural similarity and aromatic interactions as a common inhibition mechanism. *Chem Biol Drug Des.* 2006;67(1):27-37.

34. Schutz AK, Soragni A, Hornemann S, Aguzzi A, Ernst M, Bockmann A, et al. The amyloid-Congo red interface at atomic resolution. *Angew Chem Int Ed Engl.* 2011;50(26):5956-60.

35. Cegelski L, Pinkner JS, Hammer ND, Cusumano CK, Hung CS, Chorell E, et al. Small-molecule inhibitors target *Escherichia coli* amyloid biogenesis and biofilm formation. *Nat Chem Biol.* 2009;5(12):913-9.

36. Nenninger AA, Robinson LS, Hammer ND, Epstein EA, Badtke MP, Hultgren SJ, et al. CsgE is a curli secretion specificity factor that prevents amyloid fibre aggregation. *Molecular Microbiology.* 2011;81(2):486-99.